Chapter 8. Chemical Dynamics

Chemical dynamics is a field in which scientists study the rates and mechanisms

of chemical reactions. It also involves the study of how energy is transferred among

molecules as they undergo collisions in gas-phase or condensed-phase environments.

Therefore, the experimental and theoretical tools used to probe chemical dynamics must

be capable of monitoring the chemical identity and energy content (i.e., electronic,

vibrational, and rotational state populations) of the reacting species. Moreover, because

the rates of chemical reactions and energy transfer are of utmost importance, these tools

must be capable of doing so on time scales over which these processes, which are often

very fast, take place. Let us begin by examining many of the most commonly employed

theoretical models for simulating and understanding the processes of chemical dynamics.

I. Theoretical Tools for Studying Chemical Change and Dynamics

A. Transition State Theory

The most successful and widely employed theoretical approach for studying reaction

rates involving species that are undergoing reaction at or near thermal-equilibrium

conditions is the transition state theory (TST) of Eyring. This would not be a good way to

model, for example, photochemical reactions in which the reactants do not reach thermal

equilibrium before undergoing significant reaction progress. However, for most thermal reactions, it is remarkably successful.

In this theory, one views the reactants as undergoing collisions that act to keep all of their degrees of freedom (translational, rotational, vibrational, electronic) in thermal equilibrium. Among the collection of such reactant molecules, at any instant of time, some will have enough internal energy to access a transition state (TS) on the Born-Oppenheimer ground state potential energy surface. Within TST, the rate of progress from reactants to products is then expressed in terms of the concentration of species that exist near the TS multiplied by the rate at which these species move through the TS region of the energy surface.

The concentration of species at the TS is, in turn, written in terms of the equilibrium constant expression of statistical mechanics discussed in Chapter 7. For example, for a bimolecular reaction A + B   C passing through a TS denoted AB*, one writes the concentration (in molecules per unit volume) of AB* species in terms of the concentrations of A and of B and the respective partition functions as

$$[AB^*] = (q_{AB^*}/V)/\{(q_A/V)(q_B/V)\} \; [A] \; [B].$$

There is, however, one aspect of the partition function of the TS species that is specific to this theory. The q_{AB*} contains all of the usual translational, rotational, vibrational, and electronic partition functions that one would write down, as we did in Chapter 7, for a conventional AB molecule except for one modification. It does not contain a $\{\exp(-h\nu_j/2kT)/(1-\exp(-h\nu_j/kT))\}$ vibrational contribution for motion along the one internal coordinate corresponding to the reaction path.

Transition Structure A

Second Order Saddle Point

Transition Structure B

Minimum for Product A

Minimum for Product B

Second Order Saddle Point
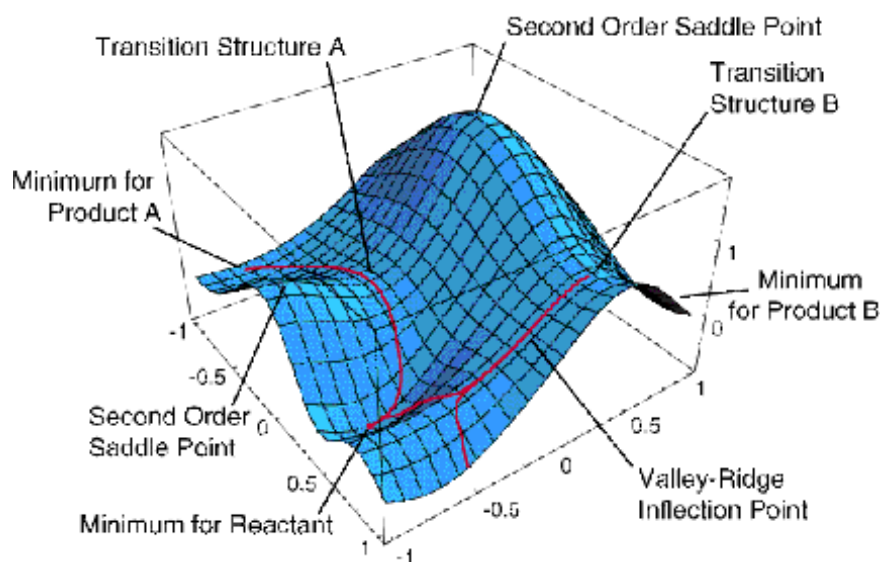
Valley-Ridge Inflection Point

Minimum for Reactant

Figure 8.1 Typical Potential Energy Surface in Two Dimensions Showing Local Minima, Transition States and Paths Connecting Them.

In the vicinity of the TS, the reaction path can be identified as that direction along which the PES has negative curvature; along all other directions, the energy surface is positively curved. For example, in Fig. 8.1, a reaction path begins at Transition Structure B and is directed "downhill". More specifically, if one knows the gradients $\{(\partial E/\partial s_k)\}$ and

Hessian matrix elements $\{ H_{j,k} = \partial^2 E/\partial s_j \partial s_k \}$ of the energy surface at the TS, one can express the variation of the potential energy along the 3N Cartesian coordinates $\{s_k\}$ of the molecule as follows:

$$E(s_k) = E(0) + \sum_k (\partial E/\partial s_k) s_k + 1/2 \sum_{j,k} s_j H_{j,k} s_k + \ldots$$

where $E(0)$ is the energy at the TS, and the $\{s_k\}$ denote displacements away from the TS geometry. Of course, at the TS, the gradients all vanish because this geometry corresponds to a stationary point. As we discussed in the Background Material, the Hessian matrix $H_{j,k}$ has 6 zero eigenvalues whose eigenvectors correspond to overall translation and rotation of the molecule. This matrix has 3N-7 positive eigenvalues whose eigenvectors correspond to the vibrations of the TS species, as well as one negative eigenvalue. The latter has an eigenvector whose components $\{s_k\}$ along the 3N Cartesian coordinates describe the direction of the reaction path as it begins its journey from the TS backward to reactants (when followed in one direction) and onward to products (when followed in the opposite direction). Once one moves a small amount along the direction of negative curvature, the reaction path is subsequently followed by taking infinitesimal "steps" downhill along the gradient vector **g** whose 3N components are $(\partial E/\partial s_k)$. Note that once one has moved downhill away from the TS by taking the initial step along the negatively curved direction, the gradient no longer vanishes because one is no longer at the stationary point.

Returning to the TST rate calculation, one therefore is able to express the concentration [AB*] of species at the TS in terms of the reactant concentrations and a

ratio of partition functions. The denominator of this ratio contains the conventional partition functions of the reactant molecules and can be evaluated as discussed in Chapter 7. However, the numerator contains the partition function of the TS species but with one vibrational component missing (i.e., $q_{vib} = \prod_{k=1,3N-7} \{\exp(-h\nu_j/2kT)/(1- \exp(-h\nu_j/kT))\}$). Other than the one missing q_{vib}, the TS's partition function is also evaluated as in Chapter 7. The motion along the reaction path coordinate contributes to the rate expression in terms of the frequency (i.e., how often) with which reacting flux crosses the TS region given that the system is in near-thermal equilibrium at temperature T.

To compute the frequency with which trajectories cross the TS and proceed onward to form products, one imagines the TS as consisting of a narrow region along the reaction coordinate s; the width of this region we denote δs. We next ask what the classical weighting factor is for a collision to have momentum p_s along the reaction coordinate. Remembering our discussion of such matters in Chapter 7, we know that the momentum factor entering into the classical partition function for translation along the reaction coordinate is $(1/h) \exp(-p_s^2/2\mu kT) dp_s$. Here, μ is the mass factor associated with the reaction coordinate s. We can express the rate or frequency at which such trajectories pass through the narrow region of width δs as $(p_s/\mu \delta s)$, with p_s/μ being the speed of passage (cm s^{-1}) and $1/\delta s$ being the inverse of the distance that defines the TS region. So, $(p_s/\mu \delta s)$ has units of s^{-1}. In summary, we expect the rate of trajectories moving through the TS region to be

$$(1/h) \exp(-p_s^2/2\mu kT) \, dp_s \, (p_s/\mu \delta s).$$

However, we still need to integrate this over all values of p_s that correspond to enough energy $p_s^2/2\mu$ to access the TS's energy, which we denote E*. Moreover, we have to account for the fact that it may be that not all trajectories with kinetic energy equal to E* or greater pass on to form product molecules; some trajectories may pass through the TS but later recross the TS and return to produce reactants. Moreover, it may be that some trajectories with kinetic energy along the reaction coordinate less than E* can react by tunneling through the barrier.

The way we account for the facts that a reactive trajectory must have at least E* in energy along s and that not all trajectories with this energy will react is to integrate over only values of p_s greater than $(2\mu E^*)^{1/2}$ and to include in the integral a so-called transmission coefficient that specifies the fraction of trajectories crossing the TS that eventually proceed onward to products. Putting all of these pieces together, we carry out the integration over p_s just described to obtain:

$$(1/h) \int exp(-p_s^2/2\mu kT) \, (p_s/\mu\, \delta s) \, ds \, dp_s$$

where the momentum is integrated from $p_s = (2\mu E^*)^{1/2}$ to ∞ and the s-coordinate is integrated only over the small region δs. If the transmission coefficient is factored out of the integral (treating it as a multiplicative factor), the integral over p_s can be done and yields the following:

$$(kT/h) \, exp(-E^*/kT).$$

The exponential energy dependence is usually then combined with the partition function of the TS species that reflect this species' other 3N-7 vibrational coordinates and momenta and the reaction rate is then expressed as

$$\text{Rate} = (kT/h) [AB^*] = (kT/h) (q_{AB^*}/V)/\{(q_A/V)(q_B/V)\} [A] [B].$$

This implies that the rate coefficient k_{rate} for this bimolecular reaction is given in terms of molecular partition functions by:

$$k_{rate} = kT/h (q_{AB^*}/V)/\{(q_A/V)(q_B/V)\}$$

which is the fundamental result of TST. Once again we notice that ratios of partition functions per unit volume can be used to express ratios of species concentrations (in number of molecules per unit volume), just as appeared in earlier expressions for equilibrium constants as in Chapter 7.

The above rate expression undergoes only minor modifications when unimolecular reactions are considered. For example, in the hypothetical reaction A   B via the TS (A*), one obtains

$$k_{rate} = kT/h \{(q_{A^*}/V)/(q_A/V)\},$$

where again q_{A^*} is a partition function of A* with one missing vibrational component.

Before bringing this discussion of TST to a close, I need to stress that this theory is not exact. It assumes that the reacting molecules are nearly in thermal equilibrium, so it is less likely to work for reactions in which the reactant species are prepared in highly non-equilibrium conditions. Moreover, it ignores tunneling by requiring all reactions to proceed through the TS geometry. For reactions in which a light atoms (i.e., an H or D atom) is transferred, tunneling can be significant, so this conventional form of TST can provide substantial errors in such cases. Nevertheless, TST remains the most widely used and successful theory of chemical reaction rates and can be extended to include tunneling and other corrections as we now illustrate.

B. Variational Transition State Theory

Within the TST expression for the rate constant of a bi-molecular reaction, $k_{rate} = kT/h \, (q_{AB*}/V)/\{(q_A/V)(q_B/V)\}$ or of a uni-molecular reaction, $k_{rate} = kT/h \, \{(q_{A*}/V)/(q_A/V)\}$, the height ($E^*$) of the barrier on the potential energy surface appears in the TS species' partition function q_{AB*} or q_{A*}, respectively. In particular, the TS partition function contains a factor of the form $\exp(-E^*/kT)$ in which the Born-Oppenheimer electronic energy of the TS relative to that of the reactant species appears. This energy E^* is the value of the potential energy $E(S)$ at the TS geometry, which we denote S_0.

It turns out that the conventional TS approximation to k_{rate} over-estimates reaction rates because it assumes all trajectories that cross the TS proceed onward to products unless the transmission coefficient is included to correct for this. In the variational transition state theory (VTST), one does not evaluate the ratio of partition functions

appearing in k_{rate} at S_0, but one first determines at what geometry (S*) the TS partition function (i.e., q_{AB*} or q_{A*}) is smallest. Because this partition function is a product of (i) the exp(-E(S)/kT) factor as well as (ii) 3 translational, 3 rotational, and 3N-7 vibrational partition functions (which depend on S), the value of S for which this product is smallest need not be the conventional TS value S_0. What this means is that the location (S*) along the reaction path at which the free-energy reaches a saddle point is not the same the location S_0 where the Born-Oppenheimer electronic energy E(S) has its saddle. This interpretation of how S* and S_0 differ can be appreciated by recalling that partition functions are related to the Helmholtz free energy A by q = exp(-A/kT); so determining the value of S where q reaches a minimum is equivalent to finding that S where A is at a maximum.

So, in VTST, one adjusts the "dividing surface" (through the location of the reaction coordinate S) to first find that value S* where k_{rate} has a minimum. One then evaluates both E(S*) and the other components of the TS species partition functions at this value S*. Finally, one then uses the k_{rate} expressions given above, but with S taken at S*. This is how VTST computes reaction rates in a somewhat different manner than does the conventional TST. As with TST, the VTST, in the form outlined above, does not treat tunneling and the fact that not all trajectories crossing S* proceed to products. These corrections still must be incorporated as an "add-on" to this theory (i.e., in the   factor) to achieve high accuracy for reactions involving light species (recall from the Background Material that tunneling probabilities depend exponentially on the mass of the tunneling particle).

C. Reaction Path Hamiltonian Theory

Let us review what the reaction path is as defined above. It is a path that

i. begins at a transition state (TS) and evolves along the direction of negative curvature on the potential energy surface (as found by identifying the eigenvector of the Hessian matrix $H_{j,k} = \partial^2 E/\partial s_k \partial s_j$ that belongs to the negative eigenvalue);

ii. moves further downhill along the gradient vector **g** whose components are $g_k = \partial E/\partial s_k$,

iii. terminates at the geometry of either the reactants or products (depending on whether one began moving away from the TS forward or backward along the direction of negative curvature).

The individual "steps" along the reaction coordinate can be labeled S_0, S_1, S_2, ... S_P as they evolve from the TS to the products (labeled S_P) and S_{-R}, S_{-R+1}, ...S_0 as they evolve from reactants (S_{-R}) to the TS. If these steps are taken in very small (infinitesimal) lengths, they form a continuous path and a continuous coordinate that we label S.

At any point S along a reaction path, the Born-Oppenheimer potential energy surface E(S), its gradient components $g_k(S) = (\partial E(S)/\partial s_k)$ and its Hessian components $H_{k,j}(S) = (\partial^2 E(S)/\partial s_k \partial s_j)$ can be evaluated in terms of derivatives of E with respect to the 3N Cartesian coordinates of the molecule. However, when one carries out reaction path dynamics, one uses a different set of coordinates for reasons that are similar to those that arise in the treatment of normal modes of vibration as given in the Background Material. In particular, one introduces 3N mass-weighted coordinates $x_j = s_j (m_j)^{1/2}$ that are related to the 3N Cartesian coordinates s_j in the same way as we saw in the Background Material.

The gradient and Hessian matrices along these new coordinates $\{x_j\}$ can be evaluated in terms of the original Cartesian counterparts:

$$g_k'(S) = g_k(S) \, (m_k)^{-1/2}$$

$$H_{j,k}' = H_{j,k} \, (m_j m_k)^{-1/2}.$$

The eigenvalues $\{\omega_k^2\}$ and eigenvectors $\{v_k\}$ of the mass-weighted Hessian H' can then be determined. Upon doing so, one finds

i.   6 zero eigenvalues whose eigenvectors describe overall rotation and translation of the molecule;

ii.   3N-7 positive eigenvalues $\{\omega_K^2\}$ and eigenvectors v_K along which the gradient g has zero (or nearly so) components;

iii.   and one eigenvalue ω_S^2 (that may be positive, zero, or negative) along whose eigenvector v_S the gradient g has its largest component.

The one unique direction along v_S gives the direction of evolution of the reaction path (in these mass-weighted coordinates). All other directions (i.e., within the space spanned by the 3N-7 other vectors $\{v_K\}$) possess zero gradient component and positive curvature. This means that at any point S on the reaction path being discussed

i.   one is at a local minimum along all 3N-7 directions $\{v_K\}$ that are transverse to the reaction path direction (i.e., the gradient direction);

ii.   one can move to a neighboring point on the reaction path by moving a small (infinitesimal) amount along the gradient.

In terms of the 3N-6 mass-weighted Hessian's eigen-mode directions ($\{\mathbf{v}_K\}$ and $\mathbf{v}_S$), the potential energy surface can be approximated, in the neighborhood of each such point on the reaction path S, by expanding it in powers of displacements away from this point. If these displacements are expressed as components

i. X_k along the 3N-7 eigenvectors $\mathbf{v}_K$ and

ii.   S along the gradient direction $\mathbf{v}_S$,

one can write the Born-Oppenheimer potential energy surface locally as:

$$E = E(S) + \mathbf{v}_S \ S + 1/2 \ _S^2 \ S^2 + \ _{K=1,3N-7} 1/2 \ _K^2 \ X_K^2 .$$

Within this local quadratic approximation, E describes a sum of harmonic potentials along each of the 3N-7 modes transverse to the reaction path direction. Along the reaction path, E appears with a non-zero gradient and a curvature that may be positive, negative, or zero.

The eigenmodes of the local (i.e., in the neighborhood of any point S along the reaction path) mass-weighted Hessian decompose the 3N-6 internal coordinates into 3N-7 along which E is harmonic and one (S) along which the reaction evolves. In terms of these same coordinates, the kinetic energy T can also be written and thus the classical Hamiltonian H = T + V can be constructed. Because the coordinates we use are mass-weighted, in Cartesian form the kinetic energy T contains no explicit mass factors:

$$T = 1/2 \ _j m_j \ (ds_j/dt)^2 = 1/2 \ _j \ (dx_j/dt)^2 .$$

This means that the momenta conjugate to each (mass-weighted) coordinate x_j, obtained in the usual way as $p_j = \partial[T-V]/\partial(dx_j/dt) = dx_j/dt$, all have identical (unit) mass factors associated with them.

To obtain the working expression for the reaction path Hamiltonian (RPH), one must transform the above equation for the kinetic energy T by replacing the 3N Cartesian mass-weighted coordinates $\{x_j\}$ by

i.   the 3N-7 eigenmode displacement coordinates X_j,

ii.   the reaction path displacement coordinate S, and

iii.   3 translation and 3 rotational coordinates.

The 3 translational coordinates can be separated and ignored (because center-of-mass energy is conserved) in further consideration. The 3 rotational coordinates do not enter into the potential E, but they do appear in T. However, it is most common to ignore their effects on the dynamics that occurs in the internal-coordinates; this amounts to ignoring the effects of overall centrifugal forces on the reaction dynamics. We will proceed with this approximation in mind.

Although it is tedious to perform the coordinate transformation of T outlined above, it has been done and results in the following form for the RPH:

$$H = \sum_{K=1,3N-7} 1/2[p_K^2 + \omega_K^2(S)] + E(S) + 1/2\ [p_S - \sum_{K,K'=1,3N-7} p_K\ X_{K'}\ B_{K,K'}]^2/(1+F)$$

where

13

$$(1+F) = [1 + \sum_{K=1,3N-7} X_K B_{K,S}]^2.$$

In the absence of the so-called dynamical coupling factors $B_{K,K'}$ and $B_{K,S}$, this expression for H describes

(1) 3N-7 harmonic-oscillator Hamiltonia $1/2[p_K^2 + \omega_K^2(S)]$ each of which has a locally defined frequency $\omega_K(S)$ that varies along the reaction path (i.e., is S-dependent);

(2) a Hamiltonian $1/2\ p_S^2 + E(S)$ for motion along the reaction coordinate S with E(S) serving as the potential.

In this limit (i.e., with the B factors "turned off"), the reaction dynamics can be simulated in what is termed a "vibrationally adiabatic" manner by

i.   placing each transverse oscillator into a quantum level v_K that characterizes the reactant's population of this mode;

ii.   assigning an initial momentum $p_S(0)$ to the reaction coordinate that is characteristic of the collision to be simulated (e.g., $p_S(0)$ could be sampled from a Maxwell-Boltzmann distribution if a thermal reaction is of interest, or $p_S(0)$ could be chosen equal to the mean collision energy of a beam-collision experiment);

iii.   time evolving the S and p_S, coordinate and momentum using the above Hamiltonian, assuming that each transverse mode remains in the quantum state v_K that it had when the reaction began.

The assumption that v_K remains fixed, which is why this model is called vibrationally adiabatic, does not mean that the energy content of the Kth mode remains fixed because the frequencies $\omega_K(S)$ vary as one moves along the reaction path. As a result, the kinetic

14

energy along the reaction coordinate $1/2 \, p_S^2$ will change both because E(S) varies along S and because $\sum_{K=1,3N-7} \hbar \, \omega_K^2(S) \, [v_K + 1/2]$ varies along S.

Let's return now to the RPH theory in which the dynamical couplings among motion along the reaction path and the modes transverse to it are included. In the full RPH, the terms $B_{K,K'}(S)$ couple modes K and K', while $B_{K,S}(S)$ couples the reaction path to mode K. These couplings are how energy can flow among these various degrees of freedom. Explicit forms for the $B_{K,K'}$ and $B_{K,S}$ factors are given in terms of the eigenvectors $\{\mathbf{v}_K, \mathbf{v}_S\}$ of the mass-weighted Hessian matrix as follows:

$$B_{K,K'} = <d\mathbf{v}_K/dS| \, \mathbf{v}_{K'}>; \; B_{K,S} = <d\mathbf{v}_K/dS \, | \, \mathbf{v}_S>$$

where the derivatives of the eigenvectors $\{d\mathbf{v}_K/dS\}$ are usually computed by taking the eigenvectors at two neighboring points S and S' along the reaction path:

$$d\mathbf{v}_K/dS = \{\mathbf{v}_K(S') - \mathbf{v}_K(S))/(S'-S).$$

In summary, once a reaction path has been mapped out, one can compute, along this path, the mass-weighted Hessian matrix and the potential E(S). Given these quantities, all terms in the RPH

$$H = \sum_{K=1,3N-7} 1/2[p_K^2 + \omega_K^2(S)] + E(S) + 1/2 \, [p_S - \sum_{K,K'=1,3N-7} p_K \, X_{K'} \, B_{K,K'}]^2/(1+F)$$

are in hand.

This knowledge can, subsequently, be used to perform the propagation of a set of classical coordinates and momenta forward in time. For any initial (i.e., t = 0) momenta p_S and p_K, one can use the above form for H to propagate the coordinates { X_K, S} and momenta {p_K, p_S} forward in time. In this manner, one can use the RPH theory to follow the time evolution of a chemical reaction that begins (t = 0) with coordinates and moment characteristic of reactants under specified laboratory conditions and moves through a TS and onward to products. Once time has evolved long enough for product geometries to be realized, one can interrogate the values of $1/2[p_K^2 + {}_K^2(S)]$ to determine how much energy has been deposited into various product-molecule vibrations and of $1/2\, p_S^2$ to see what the final kinetic energy of the product fragments is. Of course, one also monitors what fraction of the trajectories, whose initial conditions are chosen to represent some experimental situation, progress to product geometries vs. returning to reactant geometries. In this way, one can determine the overall reaction probability.

D. Classical Dynamics Simulation of Rates

One can perform classical dynamics simulations of reactive events without using the reaction path Hamiltonian. Following a procedure like that outlined in Chapter 7 where condensed-media MD simulations were discussed, one can time-evolve the Newton equations of motion of the molecular reaction species using, for example, the Cartesian coordinates of each atom in the system and with either a Born-Oppenheimer surface or a parameterized functional form. Of course, it is essential for whatever

function one uses to accurately describe the reactive surface, especially near the transition state.

With each such coordinate having an initial velocity $(dq/dt)_0$ and an initial value q_0, one then uses Newton's equations written for a time step of duration Δt to propagate q and dq/dt forward in time according, for example, to the following first-order propagation formula:

$$q(t + \Delta t) = q_0 + (dq/dt)_0 \, \Delta t$$

$$dq/dt \, (t + \Delta t) = (dq/dt)_0 - \Delta t \, [(\partial E/\partial q)_0/m_q].$$

Here m_q is the mass factor connecting the velocity dq/dt and the momentum p_q conjugate to the coordinate q:

$$p_q = m_q \, dq/dt,$$

and $-(\partial E/\partial q)_0$ is the force along the coordianate q at the "initial" geometry q_0. Again, as in Chapter 7, I should note that the above formulas for propagating q and p forward in time represent only the most elementary approach to this problem. There are other, more sophisticated, numerical methods for effecting more accurate and longer-time propagations, but I will not go into them here. Rather, I wanted to focus on the basics of how these simulations are carried out.

By applying the time-propagation proecess, one generates a set of "new" coordinates q(t+ t) and new velocities dq/dt(t+ t) appropriate to the system at time t+ t. Using these new coordinates and momenta as q_0 and $(dq/dt)_0$ and evaluating the forces $-(\partial E/\partial q)_0$ at these new coordinates, one can again use the Newton equations to generate another finite-time-step set of new coordinates and velocities. Through the sequential application of this process, one generates a sequence of coordinates and velocities that simulate the system's dynamical behavior.

In using this kind of classical trajectory approach to study chemical reactions, it is important to choose the initial coordinates and momenta in a way that is representative of the experimental conditions that one is attempting to simulate. The tools of statistical mechanics discussed in Chapter 7 guide us in making these choices. When one attempts, for example, to simulate the reactive collisions of an A atom with a BC molecule to produce AB + C, it is not appropriate to consider a single classical (or quantal) collision between A and BC. Why? Because in any laboratory setting,

1. The A atoms are probably moving toward the BC molecules with a distribution of relative speeds. That is, within the sample of molecules (which likely contains 10^{10} or more molecules), some A + BC pairs have low relative kinetic energies when they collide, and others have higher relative kinetic energies. There is a probability distribution $P(E_{KE})$ for this relative kinetic energy that must be properly sampled in choosing the initial conditions.

2. The BC molecules may not all be in the same rotational (J) or vibrational (v) state. There is a probability distribution function P(J,v) describing the fraction of BC molecules that are in a particular J state and a particular v state. Initial values of the BC molecule's

internal vibrational coordinate and momentum as well as its orientation and rotational

angular momentum must be selected to represent this P(J,v).

3. When the A and BC molecules collide with a relative motion velocity vector v, they do

not all hit "head on". Some collisions have small impact parameter b (the closest distance

from A to the center of mass of BC if the collision were to occur with no attractive or

repulsive forces), and some have large b-values (see Fig. 8.2). The probability function

for these impact parameters is $P(b) = 2 \pi b \, db$, which is simply a statement of the

geometrical fact that larger b-values have more geometrical volume element than smaller
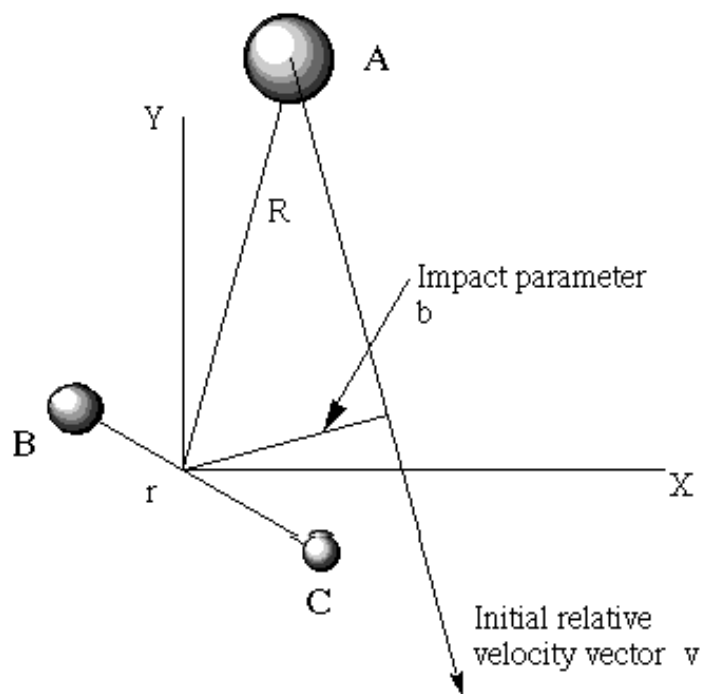
b-values.

Figure 8.2 Coordinates Needed to Characterize an Atom-Diatom Collision Showing the

Impact Parameter b.

So, to simulate the entire ensemble of collisions that occur between A atoms and

BC molecules in various J, v states and having various relative kinetic energies E_{KE} and

impact parameters b, one must:

1. run classical trajectories (or quantum propagations) for a large number of J, v, E_{KE} ,

and b values,

2. with each such trajectory assigned an overall weighting (or importance) of

$$P_{total} = P(E_{KE}) \, P(J,v) \, 2 \, b \, db.$$

After such an ensemble of trajectories representative of an experimental condition

has been carried out, one has available a great deal of data. This data includes knowledge

of what fraction of the trajectories produced final geometries characteristic of products,

so the net reaction probability can be calculated. In addition, the kinetic and potential

energy content of the internal (vibrational and rotational) modes of the product molecules

can be interrogated and used to compute probabilities for observing products in these

states. This is how classical dynamics simulations allow us to study chemical reactions

and/or energy transfer.

E. RRKM Theory

Another theory that is particularly suited for studying uni-molecular decomposition

reactions is named after the four scientists who developed it- Rice, Ramsperger, Kassel,

and Marcus. To use this theory, one imagines an ensemble of molecules that have been

"activated" to a state in which they possess a specified total amount of internal energy E of which an amount E^*_{rot} exists as rotational energy and the remainder as internal vibrational energy.

The mechanism by which the molecules become activated could involve collisions or photochemistry. It does not matter as long as enough time has passed to permit one to reasonably assume that these molecules have the energy $E-E^*_{rot}$ distributed randomly among all their internal vibrational degrees of freedom. When considering thermally activated unimolecular decomposition of a molecule, the implications of such assumptions are reasonably clear. For photochemically activated unimolecular decomposition processes, one usually also assumes that the molecule has undergone radiationless relaxation and returned to its ground electronic state but in a quite vibrationally "hot" situation. That is, in this case, the molecule contains excess vibrational energy equal to the energy of the optical photon used to excite it. Finally, when applied to bimolecular reactions, one assumes that collision between the two fragments results in a long-lived complex. The lifetime of this intermediate must be long enough to allow the energy $E-E^*_{rot}$, which is related to the fragments' collision energy, to be randomly distributed among all vibrational modes of the collision complex.

For bimolecular reactions that proceed "directly" (i.e., without forming a long-lived intermediate), one does not employ RRKM-type theories because their primary assumption of energy randomization almost certainly would not be valid in such cases.

The RRKM expression of the unimolecular rate constant for activated molecules A* (i.e., either a long-lived complex formed in a bimolecular collision or a "hot" molecule) dissociating to products through a transition state, A*   TS   P, is

$$k_{rate} = G(E-E_0 -E'_{tot})/(N(E-E^*_{rot}) h).$$

Here, the total energy E is related to the energies of the activated molecules by

$$E = E^*_{rot} + E^*_{vib}$$

where E^*_{rot} is the rotational energy of the activated molecule and E^*_{vib} is the vibrational energy of this molecule. This same energy E must, of course, appear in the transition state where it is decomposed as an amount E_0 needed to move from A* to the TS (i.e, the energy needed to reach the barrier) and vibrational (E'_{vib}) , translational (E'_{trans} along the reaction coordiate), and rotational (E'_{rot}) energies:

$$E = E_0 + E'_{vib} + E'_{trans} + E'_{rot} .$$

In the rate coefficient expression, $G(E-E_0 -E'_{rot})$ is the total sum of internal vibrational quantum states that the transition state possesses having energies up to and including $E-E_0 -E'_{rot}$. This energy is the total energy E but with the activation energy E_0 removed and the overall rotational energy E'_{rot} of the TS removed. The quantity $N(E-E^*_{rot})$ is the density of internal vibrational quantum states (excluding the mode describing the reaction coordinate) that the activated molecule possesses having an energy between $E-E^*_{rot}$ and $E-E^*_{rot} + dE$. In this expression, the energy $E-E^*_{rot}$ is the total energy E with the rotational energy E^*_{rot} of the activated species removed.

In the most commonly employed version of RRKM theory, the rotational energies of the activated molecules E^*_{rot} and of the TS E'_{rot} are assumed to be related by

$$E^*_{rot} - E'_{rot} = J(J+1) h^2/8 \pi^2 \{1/I^* - 1/I'\} = E^*_{rot} \{1 - I^*/I'\}.$$

Here I^* and I' are the average (taken over the three eigenvalues of the moment inertia tensors) moments of inertia of the activated molecules and TS species, respectively. The primary assumption embodied in the above relationship is that the rotational angular momenta of the activated and TS species are the same, so their rotational energies can be related, as expressed in the equation, to changes in geometries as reflected in their mometns of inertia. Because RRKM theory assumes that the vibrational energy is randomly distributed, its fundamental rate coefficient equation

$k_{rate} = G(E-E_0 - E'_{tot})/(N(E-E^*_{rot}) h)$ depends on the total energy E, the energy E_0 required to access the TS, and the amount of energy contained in the rotational degrees of freedom that is thus not available to the vibrations.

To implement a RRKM rate coefficient calculation, one must know

(i)   the total energy E available,

(ii) the barrier energy E_0,

(iii) the geometries (and hence the moments of inertia I^* and I') of the activated

        molecules and of the TS, respectively,

(iv) the rotational energy E^*_{rot} of the activated molecules, as well as

(v)   all 3N-6 vibrational energies of the activated molecules and all 3N-7 vibrational

        energiers of the TS (i.e., excluding the reaction coordinate).

The rotational energy of the TS species can then be related to that of the activated molecules through $E^*_{rot} - E'_{rot} = E^*_{rot}\{1 - I^*/I'\}$.

To simulate an experiment in which the activated molecules have a thermal distribution of rotational energies, the RRKM rate constant is computed for a range of E^*_{rot} values and then averaged over E^*_{rot} using the thermal Boltzmann population $(2J+1) \exp(-J(J+1)h^2/(8 \pi^2 I^* kT))$ as a weighting factor. This can be carried out, for example, using the MC process for selecting rotational J values. This then produces a rate constant for any specified total energy E. Alternatively, to simulate experiments in which the activated species are formed in bimolecular collisions at a specified energy E, the RRKM rate coefficient is computed for a range of E^*_{rot} values with each E^*_{rot} related to the collisional impact parameter b that we discussed earlier. In that case, the collisional angular momentum J is given as $J = \mu\, v\, b$, where v is the collision speed (related to the collision energy) and μ is the reduced mass of the two colliding fragments. Again using $E^*_{rot} - E'_{rot} = E^*_{rot}\{1 - I^*/I'\}$ the TS rotational energy can be related to that of the activated species. Finally, the RRKM rate coefficient is evaluated by averaging the result over a series of impact parameters b (each of which implies a J value and thus an E^*_{rot}) with $2\pi b\, db$ as the weighting factor.

The evaluation of the sum of states $G(E-E_0 - E'_{tot})$ and the density of states $N(E-E^*_{rot})$ that appear in the RRKM expression is usually carried out using a state-counting algorithm such as that implemented by Beyer and Swinehart (Commun. Assoc. Comput. Machin. <u>16</u>, 372 (1973)). This algorithm uses knowledge of the 3N-6 harmonic vibrational frequencies of the activated molecules and the 3N-7 frequencies of the TS and determines how many ways a given amount of energy can be distributed among these

modes. By summing over all such distributions for energy varying from zero to E, the algorithm determines G(E). By taking the difference G(E+ E) – G(E), it determines N(E) E.

F. Correlation Function Expressions for Rates

Recall from Chapter 6 that rates of photon absorption can, in certain circumstances, be expressed either (a) in terms of squares of transition dipole matrix elements connecting each initial state $_i$ to each final state $_f$,

$$| \mathbf{E}_0 \bullet <{}_f | \mu | {}_i> |^2$$

or (b) in terms of the equilibrium average of the product of a transition dipole vector at time t=0 dotted into this same vector at another time t

$$_i\ {}_i <{}_i | \mathbf{E}_0 \bullet \mu\ \mathbf{E}_0 \bullet \mu\,(t) | {}_i>$$

That is, these rates can be expressed either in a state-to-state manner or in a time-dependent correlation function framework. In Chapter 7, this same correlation function approach was examined further.

In an analogous fashion, it is possible to express chemical reaction rate constants in a time-domain language again using time correlation functions. The TST (or VTST) and RRKM expressions for the rate constant k_{rate} all involve, through the partition

functions or state densities, the reactant and transition-state energy levels and
degeneracies. These theories are therefore analogs of the state-to-state photon-absorption
rate equations.

To make the connection between the state-to-state and time-correlation function
expressions, one can begin with a classical expression for the rate constant given below:

$$k(T) = Q_r^{-1}(2 \pi \hbar)^{-L} \int dp\, dq\, e^{-\beta H(q,p)} F(p,q)\, \chi(p,q)$$

Here Q_r is the partition function of the reactant species, L is the number of coordinates
and momenta upon which the Hamiltonian H(**p,q**) depends, and β is 1/kT. The flux factor
F and the reaction probability χ are defined in terms of a dividing surface which could,
for example, be a plane perpendicular to the reaction coordinate S and located along
the reaction path that was discussed earlier in this Chapter in Section IC. Points on such
a surface can be defined by specifying one condition that the L coordinates $\{q_j\}$ must
obey, and we write this condition as

$$f(\mathbf{q}) = 0.$$

Points lying where $f(\mathbf{q}) < 0$ are classified as lying in the reactant region of coordinate
space, while those lying where $f > 0$ are in the product region. For example, if the
dividing surface is defined as mentioned above as being a plane perpendicular to the
reaction path, the function f can be written as:

$$f(\mathbf{q}) = (S - S_0).$$

Here, S is the reaction coordinate (which, of course, depends on all of the $\mathbf{q}$ variables) and S_0 is the value of S at the dividing surface. If the dividing surface is placed at the transition state on the energy surface, S_0 vanishes because the transition state is then, by convention, the origin of the reaction coordinate.

So, now we see how the dividing surface can be defined, but how are the flux F and probability constructed? The flux factor F is defined in terms of the dividing surface function $f(\mathbf{q})$ as follows:

$$F(\mathbf{p},\mathbf{q}) = d\ h(f(\mathbf{q}))/dt$$

$$= (dh/df)\ (df/dt)$$

$$= (dh/df)\ \sum_j\ \partial f/\partial q_j\ (dq_j/dt)$$

$$= \delta(f(\mathbf{q}))\ \sum_j\ \partial f/\partial q_j\ (dq_j/dt).$$

Here, $h(f(\mathbf{q}))$ is the Heaviside step function ($h(x) = 1$ if $x>0$; $h(x) = 0$ if $x < 0$), whose derivative $dh(x)/dx$ is the Dirac delta function $\delta(x)$, and the other identities follow by using the chain rule. When the dividing surface is defined in terms of the reaction path coordinate S as introduced earlier (i.e., $f(\mathbf{q}) = (S - S_0)$), the factor $\sum_j\ \partial f/\partial q_j\ (dq_j/dt)$ contains only one term when the L coordinates $\{q_j\}$ are chosen, as in the reaction path

theory, to be the reaction coordinate S and L-1 coordinates $\{q'_j\} = \mathbf{q'}$ perpendicular to the

reaction path. For such a choice, one obtains

$$\sum_j \partial f / \partial q_j \, (dq_j/dt) = dS/dt = P_S/m_S$$

where P_S is the momentum along S and m_S is the mass factor associated with S in the

reaction path Hamiltonian. So, in this case, the total flux factor F reduces to:

$$F(\mathbf{p},\mathbf{q}) = \delta(S-S_0) \, P_S/m_S.$$

We have seen exactly this construct before in Section IA where the TST expression for

the rate coefficient was developed.

The reaction probability factor $\chi(\mathbf{p},\mathbf{q})$ is defined in terms of those trajectories that

evolve, at long time $t \to \infty$, onto the product side of the dividing surface; such trajectories

obey

$$\chi(\mathbf{p},\mathbf{q}) = \lim_t h(f(\mathbf{q}(t))) = 1.$$

This long-time limit can, in turn, be expressed in a form where the flux factor again

occurs:

$$\lim_t h(f(q(t))) = \int_0 \frac{dh(f(q(t)))}{dt} dt = \int_0 F dt$$

28

In this expression, the flux F(t) pertains to coordinates **q**(t) and momenta **p**(t) at t > 0. Because of time reversibility, the integral can be extended to range from from t = -∞ to t = ∞.

Using the expressions for and for F as developed above in the equation for the rate coefficient given at the beginning of this Section allows the rate coefficient k(T) to be rewritten as follows:

$$k(T) = Q_r^{-1}(2\pi\hbar)^{-L} \int dpdq e^{-\beta H(q,p)} F(p,q) \delta(p,q)$$

$$= Q_r^{-1}(2\pi\hbar)^{-L} \int_{-\infty}^{\infty} dt \int dpdq e^{-\beta H(q,p)} F(p,q) F(p(t),q(t))$$

In this form, the rate constant k(T) appears as an equilibrium average (represented by the integral over the initial values of the variables **p** and **q** with the $Q_r^{-1}(2\pi\hbar)^{-L} \exp(-\beta H)$ weighting factor) of the time correlation function of the flux F:

$$\int_{-\infty}^{\infty} dt F(p,q) F(p(t),q(t))$$

To evaluate the rate constant in this time-domain framework for a specific chemical reaction, one would proceed as follows.

i. Run an ensemble of trajectories whose initial coordinates and momenta {**q.p**} are selected (e.g., using Monte-Carlo methods discussed in Chapter 7) from a distribution with exp(-β H) as its weighting factor.

ii. Make sure that the initial coordinates {$\mathbf{q}$} lie on the dividing surface because the flux

expression contains the δ(f($\mathbf{q}$)) factor;

iii. Monitor each trajectory to observe when it again crosses the dividing surface (i.e.,

when {$\mathbf{q}$(t)} again obeys f($\mathbf{q}$(t)) = 0; at which time the quantity

iv. F(p(t),q(t)) can be evaluated as F($\mathbf{p},\mathbf{q}$) = δ(f($\mathbf{q}$)) $\sum_j$ ∂f/∂q$_j$ (dq$_j$/dt), using the coordinates

and momenta at time t to compute these quantities.

Using a planar dividing surface attached to the reaction path at S = S$_0$ as noted

earlier allows F($\mathbf{q},\mathbf{p}$) to be calculated in terms of the initial (t=0) momentum lying along

the reaction path direction as , F($\mathbf{p},\mathbf{q}$) = δ(S-S$_0$) P$_S$/m$_S$ and permits F($\mathbf{p}$(t),$\mathbf{q}$(t)) to be

computed when the trajectory again crosses this surface at at time t as F($\mathbf{p}$(t),$\mathbf{q}$(t)) = δ(S-

S$_0$) P$_S$(t)/m$_S$. So, all that is really needed if the dividing surface is defined in this manner

is to start trajectories with S = S$_0$; to keep track of the initial momentum along S; to

determine at what times t the trajectory returns to S = S$_0$; and to form the product (P$_S$/m$_S$)

(P$_S$(t)/m$_S$) for each such time. It is in this manner that one can compute flux-flux

correlation functions and, thus, the rate coefficient.

Notice that trajectories that undergo surface re-crossings contribute negative

terms to the flux-flux correlation function computed as discussed above. That is, a

trajectory with a positive initial value of (P$_S$/m$_S$) can, at some later time t, cross the

dividing surface with a negative value of (P$_S$(t)/m$_S$) (i.e, be directed back toward

reactants). This re-crossing will contribute a negative value, via. the product (P$_S$/m$_S$)

(P$_S$(t)/m$_S$), to the total correlation function, which integrates over all times. Of course, if

this same trajectory later undergoes yet another crossing of the dividing surface at t' with

positive $P_S(t')$, it will contribute a positive term to the correlation function via. (P_S/m_S) $(P_S(t')/m_S)$. Thus, the correlation function approach to computing the rate coefficient can properly account for surface re-crossings, unlike the TST which requires one to account for such effects (and tunneling) in the transmission coefficient .

G. Wave Packet Propagation

The preceding discussion should have made it clear that it is very difficult to propagate wave functions rigorously using quantum mechanics. On the other hand, to propagate a classical trajectory is relatively straightforward. There exists a powerful tool that allows one to retain much of the computational ease and convenient interpretation of the classical trajectory approach while also incorporating quantum effects that are appropriate under certain circumstances. In this wave packet propagation approach, one begins with a quantum mechanical wave function that is characterized by two parameters that give the average value of the position and momentum along each coordinate. One then propagates not the quantum wave function but the values of these two parameters, which one assumes will evolve according to Newtonian dynamics. Let's see how these steps are taken in more detail and try to understand when such an approach is expected to work or to fail.

First, the form of the so-called wave packet quantum function is written as follows:

$$(\mathbf{q}, \mathbf{Q}, \mathbf{P}) = \prod_{J=1,N} (2 < q_J^2 >)^{-1/2} \exp[(iP_J q_J/\hbar) - (q_J - Q_J)^2/4 < q_J^2 >].$$

Here, we have a total of N coordinates that we denote $\{q_J : J = 1, N\}$. It is these

coordinates that the quantum wave function depends upon. The total wave function is a

product of terms, one for each coordinate. Notice that this wave function has two distinct

ways in which the coordinate q_J appear. First, it has a Gaussian $(\exp[-(q_J - Q_J)^2/4< q_J^2>])$

dependence centered at the values Q_J and having Gaussian width factors related to $<q_J^2>$.

This dependence tends to make the wave function's amplitude largest when q_J is close to

Q_J. Secondly, it has a form $\exp[(iP_J q_J/\hbar)]$ that looks like the travelling wave that we

encountered in the Background Material in which the coordinate q_J moves with

momentum P_J. So, these wave packet functions have built into them characteristics that

allow them to describe motion (via. the P_J) of an amplitude that is centered at Q_J with a

width given by the parameter $<q_J^2>$.

The parameters P_J and Q_J we assume in this approach to chemical dynamics will

undergo classical time evolution according to the Newton equations:

$$dQ_J/dt = P_J/m_J$$

$$dP_J/dt = - \partial E/\partial Q_J$$

where E is the potential energy surface (Born-Oppenheimer or force field) upon which

we wish to propagate the wave packet, and m_J is the mass associated with coordinate q_J.

The Q_J and P_J parameters can be shown to be the expectation values of the coordinates q_J

and momenta $-i\hbar \partial/\partial q_J$ for the above function:

$$Q_J = \int \Psi^* \, q_J \, \Psi \, d\mathbf{q},$$

$$P_J = \int \Psi^* \, (- i \hbar \, \partial / \partial q_J) \, \Psi \, d\mathbf{q}.$$

Moreover, the $\langle q_J^2 \rangle$ parameter appearing in the Gaussian part of the function can be shown to equal the dispersion or "spread" of this wave function along the coordinate q_J:

$$\langle q_J^2 \rangle = \int \Psi^* \, (q_J - Q_J)^2 \, \Psi \, d\mathbf{q}.$$

There is an important characteristic of the above Gaussian wave packet functions that we need to point out. It turns out that functions of this form:

$$\Psi(\mathbf{q}, \mathbf{Q(t)}, \mathbf{P(t)}) = \prod_{J=1,N} (2\pi \langle q_J^2 \rangle)^{-1/2} \exp[(iP_J(t) \, q_J/\hbar) - (q_J - Q_J(t))^2 / 4\langle q_J^2 \rangle]$$

can be shown to have uncertainties in q_J and in $- i \hbar \, \partial / \partial q_J$ that are as small as possible:

$$\langle (q_J - Q_J)^2 \rangle \langle (- i \hbar \, \partial / \partial q_J - P_J)^2 \rangle = \hbar^2/4.$$

The Heisenberg uncertainty relation, which is discussed in many texts dealing with quantum mechanics, says that this product of coordinate and momentum dispersions must be greater than or equal to $\hbar^2/4$. In a sense, the Gaussian wave packet function is the most

classical function that one can have because its uncertainty product is as small as possible (i.e, equals $\hbar^2/4$). We say this is the most classical possible quantum function because in classical mechanics, both the coordinate and the momentum can be known precisely. So, whatever quantum wave function allows these two variables to be least uncertain is the most classical.

To use wave packet propagation to simulate a chemical dynamics event, one begins with a set of initial classical coordinates and momenta $\{Q_J(0), P_J(0)\}$ as well as a width $<q_J^2>$ or uncertainty for each coordinate. Each width must be chosen to represent the range of that coordinate in the experiment that is to be simulated. For example, assume one were to represent the dynamics of a wave function that is prepared by photon absorption of a $v = 0$ vibrational state of the H-Cl molecule from the ground [1] state to an excited-state energy surface ($E(R)$). Such a situation is described qualitatively in Fig. 8.3. In this case, one could choose $< R^2>$ to be the half width of the $v = 0$ harmonic (or Morse) oscillator wave function $_0(R)$ of H-Cl, and take $P(0) = 0$ (because this is the average value of the momentum for $_0$) and $R(0) = R_{eq}$, the equilibrium bond length.

For such initial conditions, classical Newtonian dynamics would then be used to propagate the Q_J and P_J. In the H-Cl example, introduced above, this propagation would be performed using the excited-state energy surface for E since, for $t > 0$, the molecule is assumed to be on this surface. The total energy at which the initial wave packet it delivered to the upper surface would be dictated by the energy of the photon used to perform the excitation. In Fig. 8.3, two such examples are shown.

Once the packet is on the upper surface, its position Q and momentum P begin to change according to the Newton equations. This, in turn, causes the packet to move as

shown for several equally spaced time "steps" in Fig. 8.3 for the two different photons'

cases. At such subsequent times, the quantum wave function is then assumed, within this

model, to be given by:

$$(\mathbf{q}, \mathbf{Q(t)}, \mathbf{P(t)}) = \prod_{J=1,N} (2 \pi < q_J^2 >)^{-1/2} \exp[(iP_J(t) q_J/\hbar) - (q_J - Q_J(t))^2 / 4 < q_J^2 >].$$

That is, it is taken to be of the same form as the initial wave function but to have simply

moved its center from Q(0) to Q(t) with a momentum that has changed from P(0) to P(t).

Wave Packet Just After Absorption of Higher-Energy Photon

t=0   **t1**   **t2**   **t3**   **t4**   **t5**

t=0   **t1**   **t2**   **t3**

Excited-State Potential

Wave Packet Just After Absorption of Low-Energy Photon

Ground-State Potential
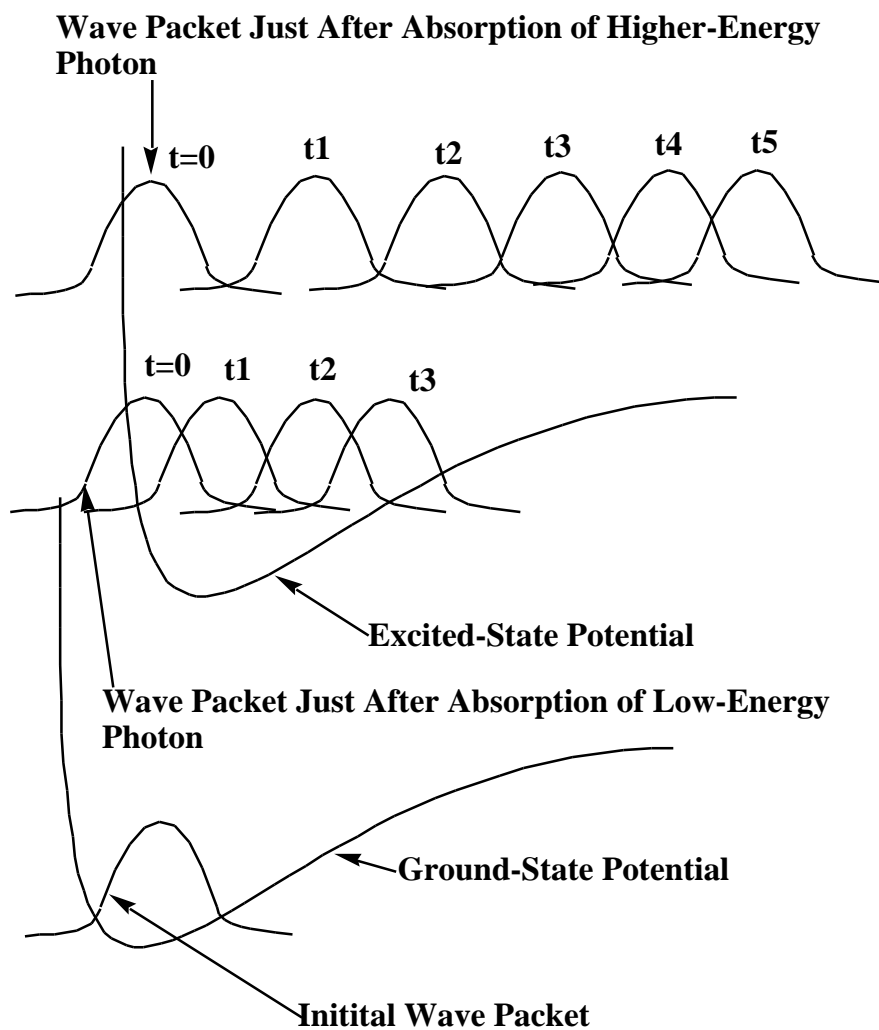
Initital Wave Packet

Figure 8.3 Propagation of Wave Packet Prepared by Absorption of Two Different

Photons.

It should be noticed that the time evolution of the wave packet shown in Fig. 8.3 displays

clear classical behavior. For example, as time evolves, it moves to large R-values and its

speed (as evidenced by the spacings between neighboring packets for equal time steps) is

large when the potential is low and small when the potential is higher. As we learned in the Background Material and in Chapter 6, the time correlation function

$$C(t) = < \Psi(q,Q(0),P(0)) | \Psi(q,Q(t),P(t))>$$

can be used to extract spectral information by Fourier transformation. For the H-Cl example considered here, this correlation function will be large at $t = 0$ but will decay in magnitude as the wave packet $\Psi(q,Q(t),P(t))$ moves to the right (at t1, t2, etc.) because its overlap with $\Psi(q,Q(0),P(0))$ becomes smaller and smaller as time evolves. This decay in $C(t)$ will occur more rapidly for the high-energy photon case because $\Psi(q,Q(t),P(t))$ moves to the right more quickly because the classical momentum $P(t)$ grows more rapidly. These dynamics will induce exponential decays in $C(t)$ (i.e., $C(t)$ will vary as $\exp(-t/\tau_1)$) at short times.

In fact, the decay of $C(t)$ discussed above produces, when $C(t)$ is Fourier transformed, the primary characteristic of the correlation function for the higher-energy photon case where dissociation ultimately occurs. In such photo-dissociation spectra, one observes a Lorentzian line shape whose width is characterized by the decay rate $(1/\tau_1)$, which, in turn, relates to the total energy of the packet and the steepness of the excited-state surface. This steepness determines how fast $P(t)$ grows, which then determines how fast the H-Cl bond fragments.

In the lower-energy photon case shown in Fig. 8.3, a qualitatively different behavior occurs in $C(t)$ and thus in the spectrum. The packet's movement to larger R causes $C(t)$ to initially undergo $\exp(-t/\tau_1)$ decay. However, as the packet moves to its

large-R turning point (shortly after time t3), it strikes the outer wall of the surface where it is reflected. Subsequently, it undergoes motion to smaller R, eventually returning to its initial location. Such recurrences, which occur on time scales that we denote τ_2, are characteristic of bound motion in contrast to the directly dissociative motion discussed earlier. This recurrence will cause C(t) to again achieve a large amplitude, but, C(t) will subsequently again undergo $\exp(-t/\tau_1)$ decay as the packet once again departs. Clearly, the correlation function will display a series of recurrences followed by exponential decays. The frequency of the recurrences is determined by the frequency with which the packet traverses from its inner to outer turning points and back again, which is proportional to $1/\tau_2$. This, of course, is the vibrational period of the H-Cl bond. So, in such bound-motion cases, the spectrum (i.e., the Fourier transform of C(t)) will display a series of peaks spaced by $(1/\tau_2)$ with the envelope of such peaks having a width determined by $1/\tau_1$.

In more complicated multi-mode cases (e.g., in molecules containing several coordinates), the periodic motion of the wave packet usually shows another feature that we have not yet discussed. Let us, for simplicity, consider a case in which only two coordinates are involved. For the wave packet to return to (or near) its initial location enough time must pass for both coordinates to have undergone an excursion to their turning points and back. For example, consider the situation in which one coordinate's vibrational frequency is ca. 1000 cm^{-1} and the other's is 300 cm^{-1}; these two modes then require ca. 1/30 ps and 1/9 ps, respectively, to undergo one complete oscillation. At t = 0, the wave packet, which is a product of two packets, $\prod_{J=1,2} (2\pi < q_J^2>)^{-1/2} \exp[(iP_J(t) q_J/\hbar) - (q_J - Q_J(t))^2/4< q_J^2>]$, one for each mode, produces a large C(t). After 1/30 ps, the first mode's coordinate has returned to its initial location, but the second mode is only 9/30 of

the way along in its periodic motion. Moreover, after 1/9 ps, the second mode's

coordinate has returned to near where it began, but now the first mode has moved away.

So, at both 1/30 ps and 1/9 ps, the correlation function will not be large because one of

the mode contribution to $C(t) = < \psi(q,Q(0),P(0)) | \psi(q,Q(t),P(t))>$ will be small.

However, after 1/3 ps, both modes' coordinates will be in positions to produce a large

value of $C(t)$; the high-frequency mode will have undergone 10 oscillations, and the

lower-frequency mode will have undergone 3 oscillations. My point in discussing this

example has been to illustrate that molecules having many coordinates can produce

spectra that display rather complicated patterns but which, in principle, can be related to

the time evolution of these coordinates using the correlation function's connection to the

spectrum.

Of course, there are problems that arise in using the wave packet function to

describe the time evolution of a molecule (or any system that should be treated using

quantum mechanics). One of the most important limitations of the wave packet approach

to be aware of relates to it inability to properly treat wave reflections. It is well know that

when a wave strikes a hard wall it is reflected by the wall. However, when, for example,

a water wave moves suddenly from a region of deep water to a much more shallow

region, one observes both a reflected and a transmitted wave. In the discussion of

tunneling resonances given in the Background Material, we also encountered reflected

and transmitted waves. Furthermore, when a wave strikes a barrier that has two or more

holes or openings in it, one observes wave fronts coming out of these openings. The

problem with the most elementary form of wave packets presented above is that each

packet contains only one "piece". It therefore can not break into two or more "pieces" as

it, for example, reflects from turning points or passes through barriers with holes.

Because such wave packets can not fragment into two or more packets that subsequently

undergo independent dynamical evolution, they are not able to describe dynamical

processes that require multiple-fragmentation events. It is primarily for this reason that

wave packet approaches to simulating dynamics are usually restricted to treating short-

time dynamics where such fragmentation of the wave packet is less likely to occur.

Prompt molecular photo-dissociation processes such as we discussed above is a good

example of such a short-time phenomenon.

H. Surface Hopping Dynamics

There are, of course, chemical reactions and energy transfer collisions in which

two or more Born-Oppenheimer energy surfaces are involved. Under such circumstances,

it is essential to have available the tools needed to describe the coupled electronic and

nuclear-motion dynamics appropriate to this situation.

The way this problem is addressed is by returning to the Schrödinger equation

before the single-surface Born-Oppenheimer approximation was made and expressing the

electronic wave function $(\mathbf{r}|\mathbf{R})$, which depends on the electronic coordinates $\{\mathbf{r}\}$ and

the nuclear coordinates $\{\mathbf{R}\}$, as:

$$(\mathbf{r}|\mathbf{R}) = \sum_J a_J(t) \; {}_J(\mathbf{r}|\mathbf{R}) \exp[-i/\hbar \int H_{J,J}(\mathbf{R}) \, dt].$$

Here, $\psi_J(\mathbf{r}|\mathbf{R})$ is the Born-Oppenheimer electronic wave function belonging to the Jth electronic state, and $H_{J,J}(\mathbf{R})$ is the expectation value of H for this state. The $a_J(t)$ are amplitudes that will eventually relate to the probability that the system is "on" the Jth surface. Substituting this expansion into the time-dependent Schrödinger equation

$$i \hbar\, \partial\psi / \partial t = H\psi$$

followed by multiplying on the left by $\psi^*_K(\mathbf{r}|\mathbf{R})$ and integrating over the electronic coordinates $\{\mathbf{r}\}$, gives an equation for the $a_K(t)$ amplitudes:

$$i \hbar\, da_K/dt = \sum_{J,K} \{ H_{K,J} - i\hbar < \psi_K|d \psi_J/dt>\} \exp[-i/\hbar \int (H_{J,J}(\mathbf{R}) - H_{K,K}(\mathbf{R})) \, dt].$$

Here, $H_{K,J}$ is the Hamiltonian matrix that couples ψ_K to ψ_J. The integral appearing in the exponential is taken from an initial time t_i when one is assumed to know that the system resides on a particular Born-Oppenheimer surface (K) up to the time t, at which the amplitude for remaining on this surface a_K as well as the amplitudes for hopping to other surfaces $\{a_J\}$ are needed. This differential equation for the amplitudes is solved numerically by starting at t_i with $a_K = 1$ and $a_{J \neq K} = 0$ and propagating the amplitudes' values forward in time.

The next step is to express $< \psi_K|d \psi_J/dt>$, using the chain rule, in terms of derivatives with respect to the nuclear coordinates $\{\mathbf{R}\}$ and the time rate of change of these coordinates:

$$< \phi_K | d\phi_J/dt> = \sum_a < \phi_K | d\phi_J/dR_a > dR_a/dt.$$

This is how a classical dynamical treatment of the nuclear motions will be introduced (i.e., by assuming that the nuclear coordinates R_a and dR_a/dt obey Newton equations). So, now the equations for the $a_K(t)$ read as follows:

$$i \hbar\, da_K/dt = \sum_{J \ne K} \{ H_{K,J} - i\hbar \sum_a dR_a/dt < \phi_K | d\phi_J/dR_a > \} \exp[-i/\hbar \int (H_{J,J}(\mathbf{R}) - H_{K,K}(\mathbf{R})) \, dt].$$

The $< \phi_K | d\phi_J/dR_a >$ are called non-adiabatic coupling matrix elements, and it is their magnitudes that play a central role in determining how efficient surface hoppings are. These matrix elements are becoming more commonly available in widely utilized quantum chemistry and dynamics computer packages (although their efficient evaluation remains a challenge that is undergoing significant study).

In addition to the above prescription for calculating amplitudes (the probabilities then being computed as $|a_J|^2$), one also needs to identify (using, perhaps the kind of strategy discussed in Chapter 3) the seam at which the surfaces of interest intersect. Let us, for example, assume that there are two surfaces that undergo such an intersection in a subspace of the 3N-6 dimensional energy surfaces $H_{1,1}$ and $H_{2,2}$, and let us denote nuclear coordinates $\{R_a\}$ that lie on this seam as obeying

$$F(R_a) = 0.$$

following the discussion of Chapter 3.

To utilize the most basic form of surface hopping theory, one proceeds as follows:

1. One begins with initial values of the nuclear coordinates $\{R_a\}$ and their velocities $\{dR_a/dt\}$ that properly characterize the kind of collision or reaction one wishes to simulate. Of course, one may have to perform many such surface hopping trajectories with an ensemble of initial conditions chosen to properly describe such an experimental situation. In addition, one specifies which electronic surface (say the Kth surface) the system is initially on.

2. For each such set of initial conditions, one propagates a classical trajectory describing the time evolution of the $\{R_a\}$ and $\{dR_a/dt\}$ on this initial surface, until such a trajectory approaches a geometry lying on the intersection seam.

3. As one is propagating the classical trajectory from t_i up to the time t_1 when it approaches the seam, one also propagates the (in this example, two) differential equations

$$i \hbar \, da_K/dt = {}_{J \, K} \{ H_{K,J} - i\hbar \, {}_a dR_a/dt < {}_K |d {}_J/dR_a> \} \exp[-i/\hbar \quad (H_{J,J}(\mathbf{R}) - H_{K,K}(\mathbf{R})) \, dt]$$

that produce the time evolution of the $\{a_J\}$ amplitudes.

4. Once the classical trajectory reaches the seam, the initial trajectory is halted and two (in the case of M coupled surfaces, M) new trajectories are initiated, one beginning (at t_1) on each of the (two in our case) coupled surfaces. Each of these new trajectories (two) are assigned a probability weighting factor computed as the square of the amplitude belonging to the surface upon which the trajectory now resides: $|a_J|^2$.

5. Each of the new trajectories is subsequently allowed to propagate from t_1 (where the nuclear coordinates are what they were just prior to diving the one initial trajectory into two (or M) trajectories) but now on different Born-Oppenheimer surfaces. This

propagation is continued until one of these trajectories again approaches a geometry on the intersection seam, at which time the trajectory hopping scheme is repeated.

Clearly, it is possible that the one initial trajectory will generate a large number of subsequent trajectories each of which is assigned an overall weighting factor taken to be the product of all of the $|a_J|^2$ probabilities associated with trajectories from which this particular trajectory was descended. It is these overall weightings that one uses to predict, one this process has been carried out long enough to allow the reaction or collision to proceed to completion, the final yield of products in each Born-Oppenheimer state. This surface-hopping algorithm remains one of the most widely used approaches to treating such coupled-state dynamics.

II. Experimental Probes of Reaction Dynamics

A. Spectroscopic Methods

To follow the rate of any chemical reaction, one must have a means of monitoring the concentrations of reactant or product molecules as time evolves. In the majority of current experiments that relate to reaction dynamics, one uses some form of spectroscopic or alternative physical probe (e.g., an electrochemical signature) to monitor

these concentrations as functions of time. Of course, in all such measurements, one must

know how the intensity of the signal detected relates to the concentration of the

molecules that cause the signal. For example, in most absorption experiments, as

illustrated in Fig. 8.4, light is passed through a sample of "thickness" L and the intensity

of the light beam in the absence of the sample I_0 and with the sample present I are

measured.

Sample of thickness L

**Intensity of
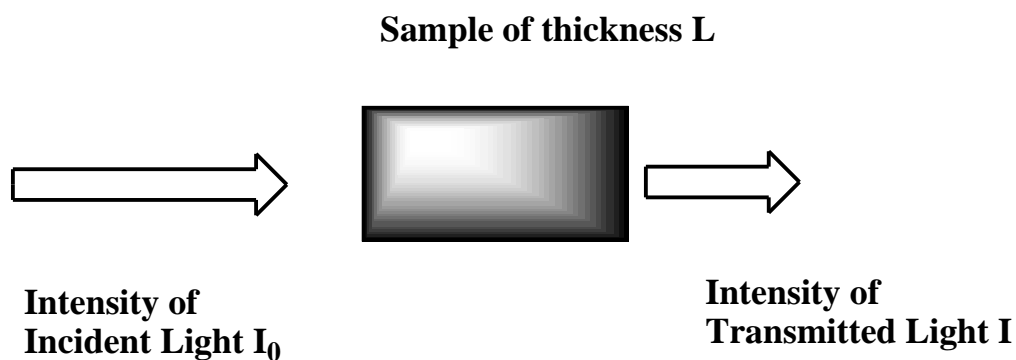Incident Light I_0**

**Intensity of
Transmitted Light I**

Figure 8.4 Typical Beer's –Law Experiment in Which a Light Beam of Intensity I_0 is

Passed Through a Sample of Thickness L.

The Beer-Lambert law:

$$\log(I_0/I) = [A] L$$

then allows the concentration [A] of the absorbing molecules to be determined, given the path length L over which absorption occurs and given the extinction coefficient ε of the absorbing molecules.

These extinction coefficients, which relate to the electric dipole matrix elements that are discussed in Chapter 6, are usually determined empirically by preparing a known concentration of the absorbing molecules and measuring the I_0/I ratio that this concentration produces in a cell of length L. For molecules and ions that are extremely reactive, this "calibration" approach to determining ε is often not feasible because one can not prepare a sample with a known and stable concentration. In such cases, one often must resort to using the theoretical expressions given in Chapter 6 (and discussed in most textbooks on molecular spectroscopy) to compute ε in terms of the wave functions of the absorbing species. In any event, one must know how the strength of the signal relates to the concentrations of the species if one wishes to monitor chemical reaction or energy transfer rates.

Because modern experimental techniques are capable of detecting molecules in particular electronic and vibration-rotation states, it has become common to use such tools to examine chemical reaction dynamics on a state-to-state level and to follow energy transfer processes, which clearly require such state-specific data. In such experiments, one seeks to learn the rate at which reactants in a specific state ψ_i react to produce products in some specific state ψ_f. One of the most common ways to monitor such state-specific rates is through a so-called "pump-probe" experiment in which

i.   A short-duration light source is used to excite reactant molecules to some specified initial state ψ_i. Usually a tunable laser is used because its narrow

frequency spread allows specific states to be pumped. The time at which this "pump" laser thus prepares the excited reactant molecules in state defines t = 0.

ii.   After a "delay time" of duration , a second light source is used to "probe" the product molecules that have been formed in various final states, $_f$. Usually, the frequency of this probe source is scanned so that one can examine populations of many such final states.

The concentrations of reactant and products molecules in the initial and final states, $_i$ and $_f$, are determined by the Beer-Lambert relation assuming that the extinction coefficients $_i$ and $_f$ for these species and states absorption are known. In the former case, the extinction coefficient relates to absorption of the pump photons to prepare reactant molecules in the specified initial state. In the latter, $_f$ refers to absorption of the product molecules that are created in the state $_f$. Carrying out a series of such final-state absorption measurements at various delay times allows one to determine the concentration of these states as a function of time.

This kind of laser pump-probe experiment is used not only to probe specific electronic or vibration/rotation states of the reactants and products but also when the reaction is fast (i.e., complete in 10^{-4}s or less). In these cases, one is not using the high frequency resolution of the laser but its fast time response. Because laser pulses of quite short duration can be generated, these tools are well suited in such fast chemical reaction studies. The reactions can be in the gas phase (e.g., fast radical reactions in the atmosphere or in explosions) or in solution (e.g., photo-induced electron transfer reactions in biological systems).

B. Beam Methods

Another approach to probing chemical reaction dynamics is to use a beam of reactant molecules A that collides with other reactants B that may also in a beam or in a "bulb" in equilibrium at some temperature T. Such crossed-beam and beam-bulb experiments are illustrated in Fig. 8.5.

Collision chamber in which A and B collide and react

Product C molecules detected exiting with velocity v" in internal state j at angle

Beam of A molecules moving with velocity v.

Beam of B molecules moving with velocity v'.

Product C molecules detected exiting with velocity v' in internal state j at angle

Beam of A molecules moving with velocity v.
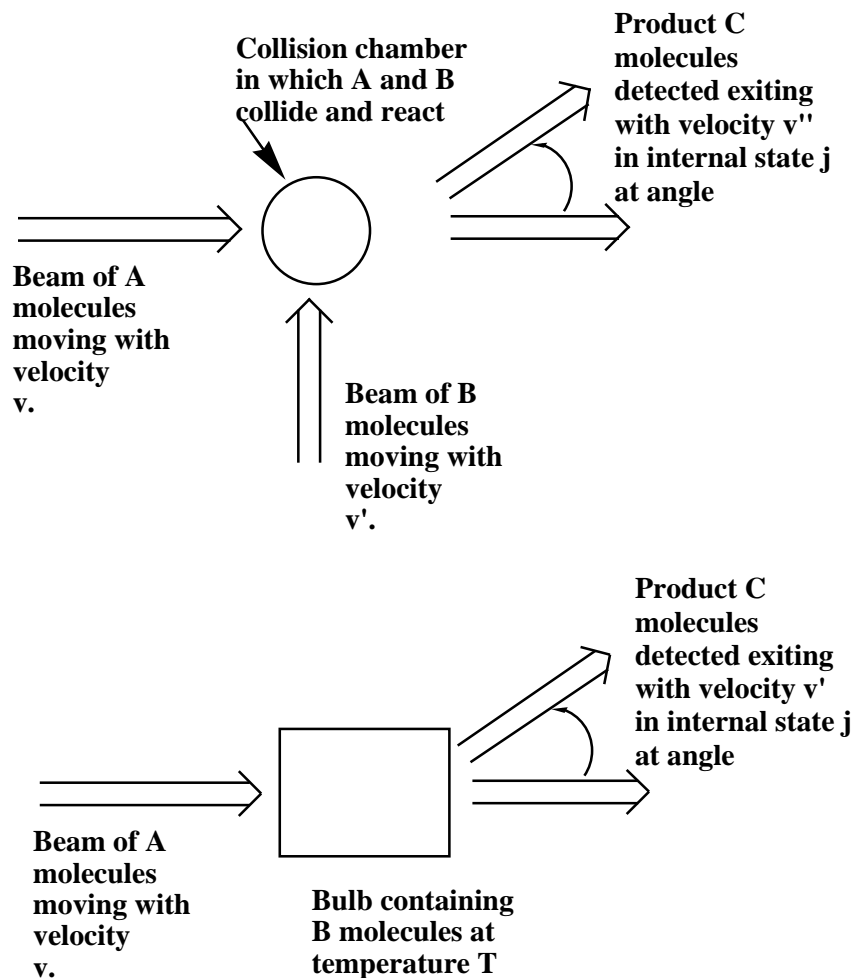
Bulb containing B molecules at temperature T

Figure 8.5 Typical Crossed-Beam and Beam-Bulb Experimental Setups.

Almost always, these beam and bulb samples contain molecules, radicals, or ions in the

gas phase, so these techniques are most prevalent in gas-phase dynamics studies.

The advantages of the crossed-beam type experiments are that:

(i) one can control the velocities, and hence the collision energies, of both reagents,

(ii) one can examine the product yield as a function of the angle   through which the products are scattered,

(iii) one can probe the velocity of the products and,

(iv) by using spectroscopic methods, one can determine the fraction of products generated in various internal (electronic/vibrational/rotational) states.

Such measurements allow one to gain very detailed information about how the reaction rate coefficient depends on collisional (kinetic) energy and where the total energy available to the products is deposited (i.e., into product translational energy or product internal energy). The angular distribution of product molecules can also give information about the nature of the reaction process. For example, if the A + B collision forms a long-lived (i.e., on rotational time scales) collision complex, the product C molecules display a very isotropic angular distribution.

In beam-bulb experiments, one is not able to gain as much detailed information because one of the reactant molecules B is not constrained to be moving with a known fixed velocity in a specified direction when the A + B   C collisions occur. Instead, the B molecules collide with A molecules in a variety of orientations and with a distribution of collision energies whose range depends on the Maxwell-Boltzmann distribution of kinetic energies of the B molecules in the bulb. The advantage of beam-bulb experiments is that one can achieve much higher collision densities than in crossed-beam experiments because the density of B molecules inside the bulb is much higher than are the densities achievable in a beam of B molecules.

There are cases in which the beam-bulb experiments can be used to determine how the reaction rate depends on collision energy even though the molecules in the bulb have

a distribution of kinetic energies. That is, if the species in the beam have much higher

kinetic energies than most of the B molecules, then the A + B collision energy is

primarily determined by the beam energy. An example of this situation is provided by so-

called guided-ion beam experiments in which a beam of ions having well-specified

kinetic energy E impinges on molecules in a bulb having a temperature T for which kT

<<E. Fig. 8.6 illustrates data that can be extracted from such an experiment.
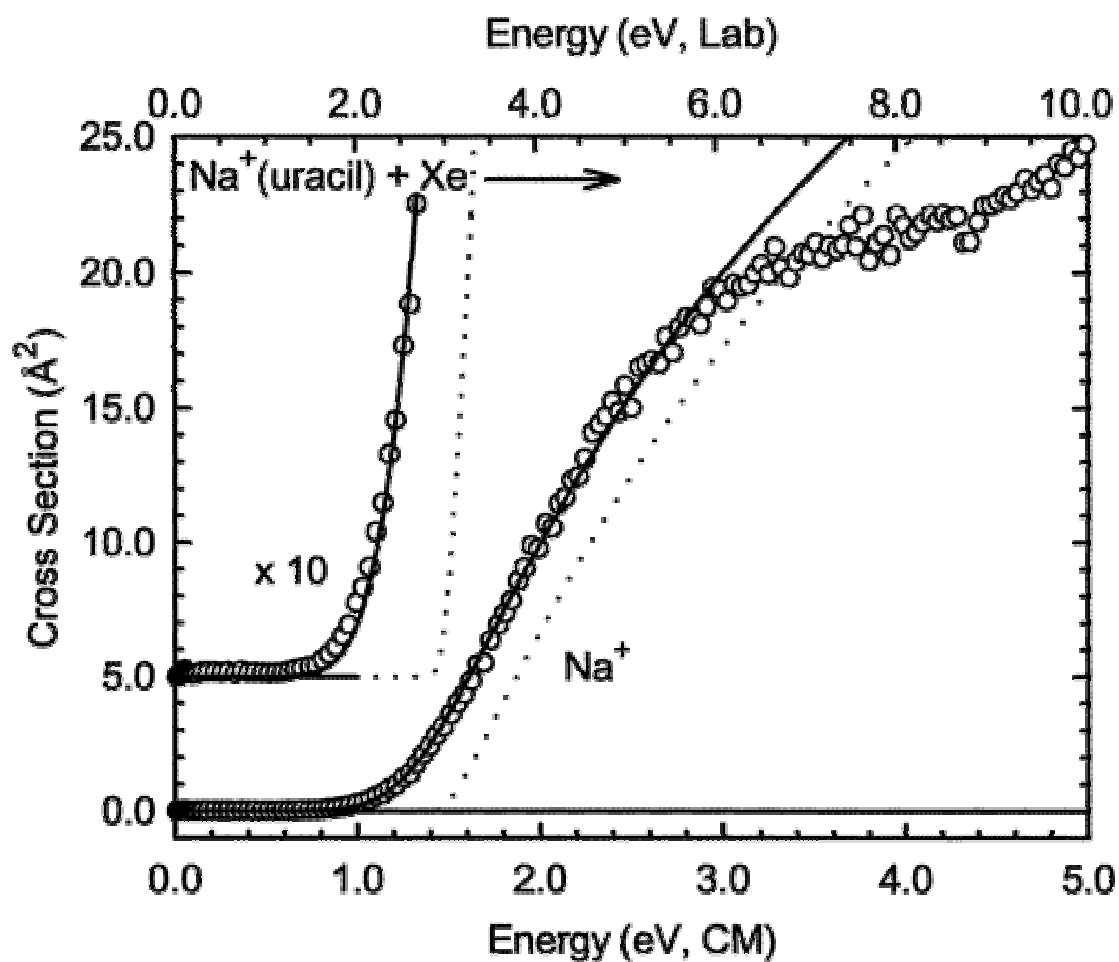
Figure 8.6 Collision-Induced Dissociation Data Showing Cross-Section as a Function of

Collision Energy.

In Fig. 8.6, we illustrate the cross-section σ (related to the bimolecular rate constant k by

σ v = k, where v is the relative collision speed) for production of Na^+ ions when a beam

of Na^+(uracil) complexes having energy E (the horizontal axis) collides with a bulb

containing Xe atoms at room temperature. In this case, the reaction is simply the

collision-induced dissociation (CID) process in which the complex undergoes

unimolecular decomposition after gaining internal energy in its collsions with Xe atoms:

$$Na^+(uracil) \quad Na^+ + uracil.$$

The primary knowledge gained in this CID experiment is the threshold energy E*; that is,

the minimum collision energy needed to effect dissociation of the Na^+(uracil) complex.

This kind of data has proven to offer some of the most useful information about bond

dissociation energies of a wide variety of species. In addition, the magnitude of the

reaction cross-section σ as a function of collision energy is a valuable product of such

experiments. These kind of CID beam-bulb experiments offer one of the most powerful

and widely used means of determining such bond-rupture energies and reaction rate

constants.

C. Other Methods

Of course, not all chemical reactions occur so quickly that they require the use of fast lasers to follow concentrations of reacting species or pump-probe techniques to generate and probe these molecules. For slower chemical reactions, one can use other methods for monitoring the relevant concentrations. These methods include electrochemistry (where the redox potential is the specie's signature) and NMR spectroscopy (where the chemical shifts of substituents are the signatures) both of whose instrumental response times would be too slow for probing fast reactions.

In addition, when the reactions under study do not proceed to completion but exist in equilibrium with a back reaction, alternative approaches can be used. The example discussed in Chapter 5 is one such case. Let us briefly review it here and again consider the reaction of an enzyme E and a substrate S to form the enzyme-substrate complex ES:

$$E + S \quad ES.$$

In the perturbation-type experiments, the equilibrium concentrations of the species are "shifted" by a small amount   by application of the perturbation, so that

$$[ES] = [ES]_{eq} -$$

$$[E] = [E]_{eq} +$$

$$[S] = [S]_{eq} + \quad .$$

Subsequently, the following rate law will govern the time evolution of the concentration change :

$$- d\ /dt = - k_r\ ([ES]_{eq} -\ ) + k_f\ ([E]_{eq} +\ )\ ([S]_{eq} +\ ).$$

Assuming that is very small (so that the term involving ^{2} cam be neglected) and using the fact that the forward and reverse rates balance at equilibrium, this equation for the time evolution of can be reduced to:

$$- d\ /dt = (k_r + k_f\ [S]_{eq} + k_f\ [E_{eq}])\ .$$

So, the concentration deviations from equilibrium will return to equilibrium exponentially with an effective rate coefficient that is equal to a sum of terms:

$$k_{eff} = k_r + k_f\ [S]_{eq} + k_f\ [E_{eq}].$$

So, by following the concentrations of the reactants or products as they return to their equilibrium values, one can extract the effective rate coefficient k_{eff}. Doing this at a variety of different initial equilibrium concentrations (e,g., $[S]_{eq}$ and $[E]_{eq}$), and seeing how k_{eff} changes, one can then determine both the forward and reverse rate constants.